Supplementary information

Note S1. Description of maximum and minimum stoichiometric numbers for RQ

The mevalonate (MVA) pathway begins with acetyl-CoA, which undergoes acetylation to form acetoacetyl-CoA. This intermediate then condenses with another acetyl-CoA molecule, catalyzed to generate HMG-CoA. HMG-CoA is subsequently reduced by HMG-CoA reductase to mevalonate, consuming 2 molecules of NADPH in the process. Mevalonate undergoes three phosphorylation steps followed by a decarboxylation, producing isopentenyl pyrophosphate (IPP) at the expense of 3 molecules of ATP. IPP serves as the skeleton and is enzymatically isomerized into dimethylallyl pyrophosphate (DMAPP). Through a series of downstream catalytic reactions, farnesene is synthesized. Based on the pathway described, the production of one molecule of farnesene requires 6 molecules of NADPH, 9 molecules of ATP and 9 molecules of acetyl-CoA. The overall reaction can be summarized as follows:

6 NADPH+ 6 H^++ 9 ATP+ 9 acetyl-CoA+6 $H_2O \rightarrow C_{15}H_{24}$+ 9 CoA+ 6 $NADP^+$+ 9 ADP+ 9 P_i+ 3 CO_2 [S1]

In *Y.lipolytica*, acetyl-CoA is transported into the cytoplasm via the citrate-pyruvate cycle, a process that requires 2 molecules of ATP, along with the generation of 1 molecule of NADPH. The relevant equations for glycolysis can be expressed as follows:

$C_3H_4O_3$+ Acetyl-CoA+ 2ATP+ $NADP^+ \rightarrow C_3H_4O_3$+ Acetyl-CoA+ 2 ADP+ 2 P_i+

NADPH [S2]

Additionally, during glycolysis, the conversion of glucose to pyruvate generates 2 molecules of ATP and 2 molecules of NADH, providing both energy and reducing equivalents for subsequent metabolic pathways. The process can be represented by the following equation:

$C_6H_{12}O_6$+ 2 ADP+ 2P_i+ 2NAD^+→ 2 $C_3H_4O_3$+2 ATP+2 NADH+2 [H] [S3]

2 [H]+O_2→ H_2O

9*[S2]+ 9*[S3]+9[S1]: 4.5 $C_6H_{12}O_6$+ 4.5 O_2→ $C_{15}H_{24}$+ 12 CO_2+ 12 H_2O [S4] (NADH, NADPH, ATP are not included in [S4])

Note S2. Determination of upper and lower boundaries associated with oxygen consumption stoichiometry analysis

To determine the stoichiometric conversion efficiency of glucose to β-farnesene in *Y. lipolytica* with respect to oxygen molecules, the following assumptions are made:

1. The fermentation process is assumed to produce only three outputs: β-farnesene, biomass, and carbon dioxide. The upper boundary corresponds to the scenario where all glucose is converted into β-farnesene and biomass, while the lower boundary assumes complete conversion into β-farnesene and carbon dioxide. This boundary definition is based on a fact that biomass has a higher degree of reduction than carbon dioxide. Consequently, glucose conversion into biomass requires the highest stoichiometric proportion of oxygen molecules involved in β-farnesene production. Conversely, glucose conversion into carbon dioxide corresponds to the lowest stoichiometric proportion of oxygen molecules used for β-farnesene synthesis.

2. For the upper boundary, at different yields (g β-farnesene/g glucose), the proportion of glucose carbon atoms converted into β-farnesene relative to the total glucose carbon atoms is determined. The remaining proportion of carbon atoms is assumed to be converted into biomass. Based on this allocation, the relevant stoichiometric equations are used to calculate the oxygen consumption required for both β-farnesene and biomass production. And the same method can be used in the calculation of lower boundary.

3. The stoichiometry of *Y. lipolytica* biomass is given as $CH_{1.6}O_{0.54}N_{0.14}$[1], with a

molecular weight of 24.2 g/mol. Additionally, it is specified that 3.14 g of biomass corresponds to the transfer of 1 electron[2]. This means that for every 0.13 moles of biomass, 1 electron is transferred.

4. The molar amount of ATP required for the growth and maintenance of 100 g of *Y. lipolytica* biomass is calculated by summing the ATP needed for growth (3978 mmol) and maintenance (25.1 mmol)[3]. These amounts are then related to the biomass, which was converted to moles using its molecular weight of 24.2 g/mol, resulting in 4.132 mol of biomass for 100 g. Finally, the ATP requirement per mole of biomass was calculated to be 0.969 mol.

For the above assumptions, it is essential to obtain the chemical equations for the conversion of glucose into these three products. Firstly, for the farnesene production in *Y. lipolytica*, the chemical equation can be described as follows. The pathway involves the citrate-oxaloacetate shuttle, which, in conjunction with acetyl-CoA ligase (ACL), provides cytosolic acetyl-CoA as the starting point for the farnesene biosynthesis pathway[4]. Therefore, the reaction can be represented as [S4]:

Furthermore, for the stoichiometric equation of glucose conversion to biomass in *Y. lipolytica*, in Hypothesis 3, since 1 mole of glucose provides 24 moles of electrons for transfer, 1 mole of glucose corresponds to 24 × 0.13 = 3.12 moles of biomass production. Through atomic conservation, the stoichiometric equation can be expressed as:

$C_6H_{12}O_6 + 2.47\ O_2 \rightarrow 3.12\ CH_{1.6}O_{0.54}N_{0.14} + 2.88\ CO_2 + 3.5\ H_2O$ [S5]

For assumption 4, it can be derived that 3.12 moles of biomass growth and maintenance require 0.969 × 3.12 = 3.02 moles of ATP production. Assuming a P/O ratio of 1.125 for ATP generation[5], the corresponding chemical equation is as follows:

$0.22\ C_6H_{12}O_6 + 1.32\ O_2 \rightarrow 1.34\ CO_2 + 1.34\ H_2O + 3.02\ ATP$ [S6]

[S5]+ [S6]: $1.22\ C_6H_{12}O_6 + 3.79\ O_2 \rightarrow 3.12\ CH_{1.6}O_{0.54}N_{0.14} + 4.22\ CO_2 + 4.84\ H_2O$ [S7]

For the generation of CO2, this can be expressed by the following equation:

$C_6H_{12}O_6 + 6\ O_2 \rightarrow 6\ CO_2 + 6\ H_2O$ [S8]

For the specific calculations of the boundary, detailed data are listed in Extended Data Table 1. To facilitate the description and computation, it is assumed that 1 mole of glucose is used as the substrate. First, from equations [S4], [S7], and [S8], the ratios of oxygen and glucose for production of farnesene, biomass, and carbon dioxide are **1**, **3.12**, and **6**, respectively.

For a glucose conversion rate of 0.001 moles, the mass conversion rate can be calculated as: Mass conversion rate = (0.001 × 204.36) / (1 × 180.1559) = 0.00113. Further calculation reveals that, at this mass conversion rate, the glucose consumption ratio for farnesene synthesis is: Farnesene glucose consumption ratio = (0.00113 × 1) / 0.252 = 0.0045 Using the O_2/Glucose stoichiometric ratio of 1 from equation (1), the oxygen consumed for farnesene synthesis is: Oxygen consumed for farnesene = 0.0045 mol of O_2. The glucose consumption ratio for biomass synthesis is: Biomass glucose consumption ratio = 1 - 0.0045 = 0.9955. Using the O_2/Glucose stoichiometric ratio of 3.01 from equation (X), the oxygen consumed for biomass synthesis is: Oxygen consumed for biomass = 0.9955 × 3.01 = 2.996455 mol of O_2. The molar ratio of farnesene to O_2 is: Molar ratio of farnesene to O_2 = 0.001 / (0.0045 + 2.996455) = 0.00033. This provides the upper boundary. Similarly, the lower boundary can be determined.

Note S3. Data cleaning and enrichment for transcriptomic sequencing

Different expressions were captured in sequencing analysis, we designed two conditions which represented high and low oxygen supply. The high oxygen supply level was represented by a stirring speed of 800 rpm and an aeration rate of 1.5 vvm, while the low oxygen supply level was represented by a stirring speed of 400 rpm and an aeration rate of 0.5 vvm. Samples were collected during the logarithmic phase (48 h, A), stationary phase (96 h, B), and late fermentation phase (168 h, C) to facilitate data analysis and interpretation. Sampling points under low oxygen supply conditions were designated as LA, LB, and LC, while those under high oxygen supply conditions were labeled HA, HB, and HC, respectively (Fig. S6a). Sequence results showed that there were significant differences between groups and correlations within groups. (Fig. S6b, c)

To quantify gene expression differences, volcano plots were generated (Fig. S6d, e, f). Differentially expressed genes (DEGs) were identified at three sampling points: the logarithmic phase (A: 179 upregulated, 241 downregulated), stationary phase (B: 121 upregulated, 121 downregulated), and late fermentation phase (C: 146 upregulated, 63 downregulated) (Fig. S6g). Sampling point A exhibited more robust growth and gene expression, correlating with a greater number of DEGs. A Venn diagram was utilized to identify overlapping differentially expressed genes across multiple sample groups and fermentation period. A total of 51 genes were found to be commonly differentially expressed between the L and H groups across points A, B, and C, further narrowing the range of differential targets (Fig. S6i). Differentially expressed genes collected by Venn analysis were filtered and corresponding to the specific functions using GO database enrichment analysis and were ranked by the value of log2(Foldchange), and the top-ranking functions were selected as further research objectives using NCBI database as a cross reference.

Note S4. Calculation of stoichiometric equation for actual production of engineered strains

To quantitatively assess sesquiterpene production efficiency, we used a stoichiometric equation for a more intuitive representation. The reaction employs glucose and oxygen as substrates, with β-farnesene, biomass, carbon dioxide, and water as products. The molar amounts of all compounds consumed and produced were determined experimentally, leading to inherent atomic conservation errors. Glucose, biomass, and β-farnesene consumption were derived from concentration measurements, while oxygen consumption and carbon dioxide production were calculated by integrating the OUR and CER curves over the entire fermentation period. H_2O was calculated based on hydrogen atom conservation. For example, the stoichiometric equation for the BY16 strain under AC-6 impeller conditions can be described as follows:

O_2 consumption: $\int_0^{240} (OUR)dt$ =17.46 mol

CO_2 production: $\int_0^{240} (OUR \times RQ)dt$ =17.12 mol

Glucose:4.01mol, Biomass:4.5mol, Farnesene:0.26mol (based on experiment determination), H_2O:17 mol (based on conservation of hydrogen atom)

Therefore, stoichiometric equation can be described as:

$$4.01\ C_6H_{12}O_6 + 17.46\ O_2 \rightarrow C_{15}H_{24} + 4.5\ CH_{1.6}O_{0.54}N_{0.14} + 17.12\ CO_2 + 17\ H_2O$$

Further quantify the equation for the generation of 1 mole of β-farnesene:

$$15.44\ C_6H_{12}O_6 + 67.22\ O_2 \rightarrow C_{15}H_{24} + 17.325\ CH_{1.6}O_{0.54}N_{0.14} + 65.91\ CO_2 + 65.45\ H_2O$$

Similarly, the stoichiometric equation for the AYL208 strain under fermentation conditions with optimized oxygen supply can be calculated.

Figure S1 Process of two-phase fermentation including seed preparation, substrate and extractant feeding.

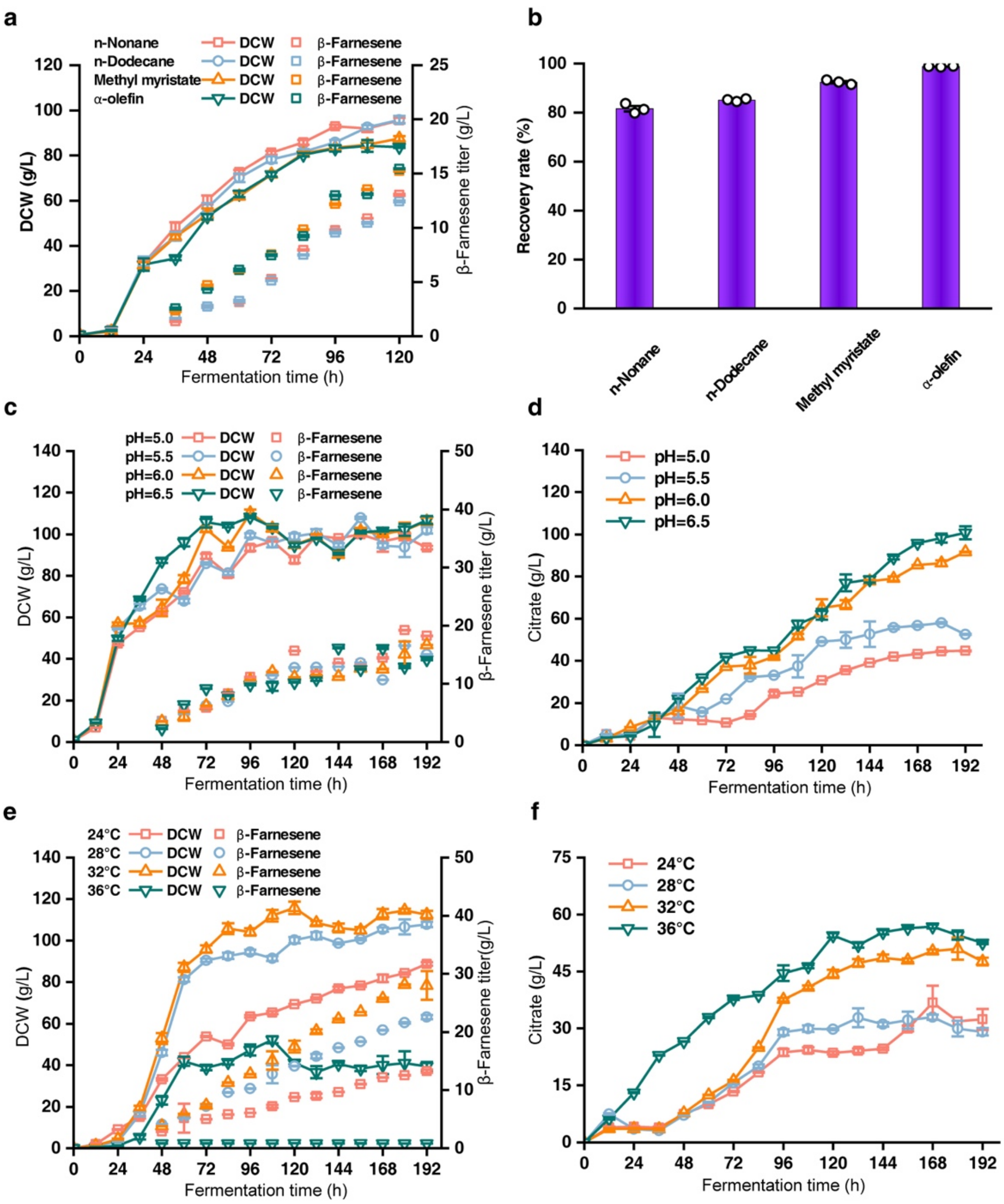

Figure S2 Optimization in fed-batch fermentation. a, Effect of different extractants on fermentation. **b,** Organic layer recovery rate on different extractants. **c,** Fermentation performance in pH 5.0, 5.5, 6.0, 6.5. **d,** Citrate accumulation in pH 5.0, 5.5, 6.0, 6.5. **e,** Fermentation performance in temperature 24°C, 28°C, 32°C, 36°C. **f,** Citrate accumulation in temperature 24°C, 28°C, 32°C, 36°C. For **a-f,** the presented data reflects the mean ± standard deviation (n = 3).

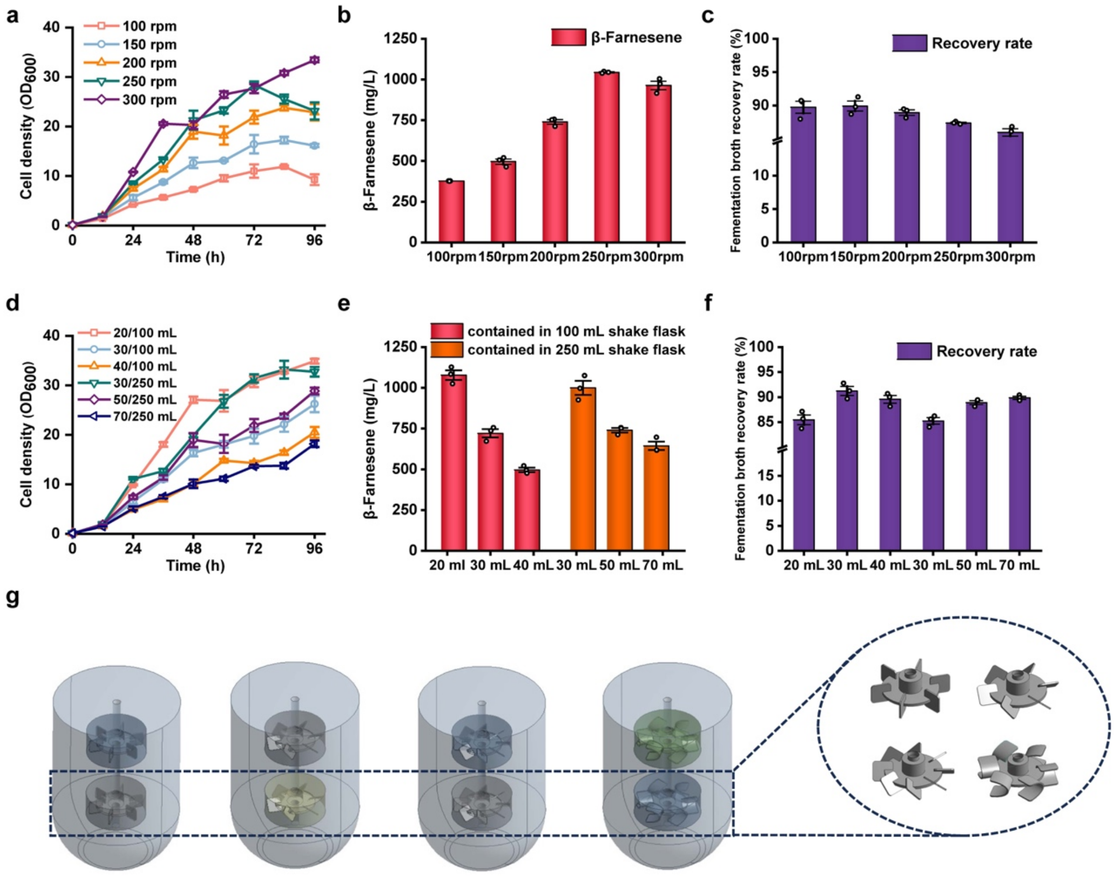

Figure S3 Effect on enhanced oxygen supply in shake flask fermentation and shape of the impellers in simulation. a, Growth performance on different agitation speeds. **b,** β-Farnesene titer. **c,** Effect of different agitation speeds on evaporation. **d,** Growth performance on different liquid charge. **e,** β-Farnesene titer. **f,** Effect of different liquid charge on evaporation. **g,** shape of the impellers in simulation (from left to right represents AS-4, AI-6, AI-8, AC-6). For **a-f,** the presented data reflects the mean ± standard deviation (n = 3).

Figure S4 β-Farnesene biosynthesis pathway and ATP/cofactor requirements

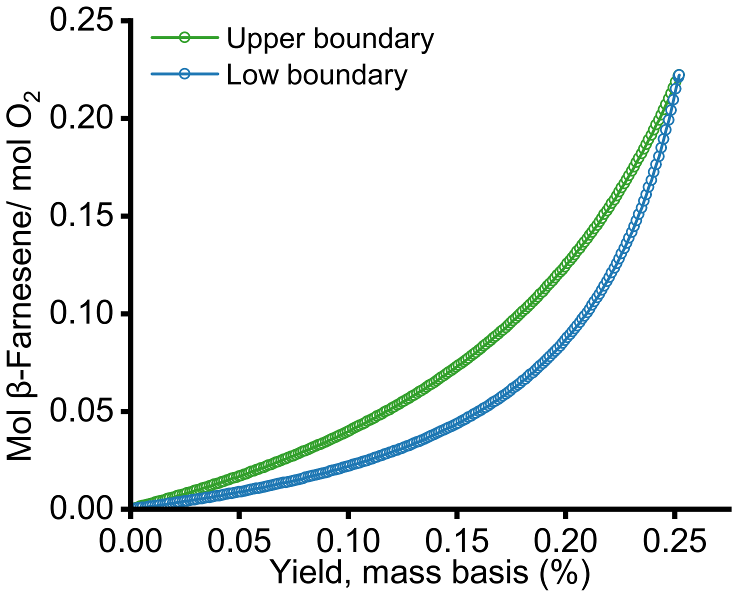

Figure S5 The theoretical boundary for β-farnesene synthesis using glucose, represented with the x-axis denoting mass yield to glucose and the y-axis denoting mole yield to oxygen.

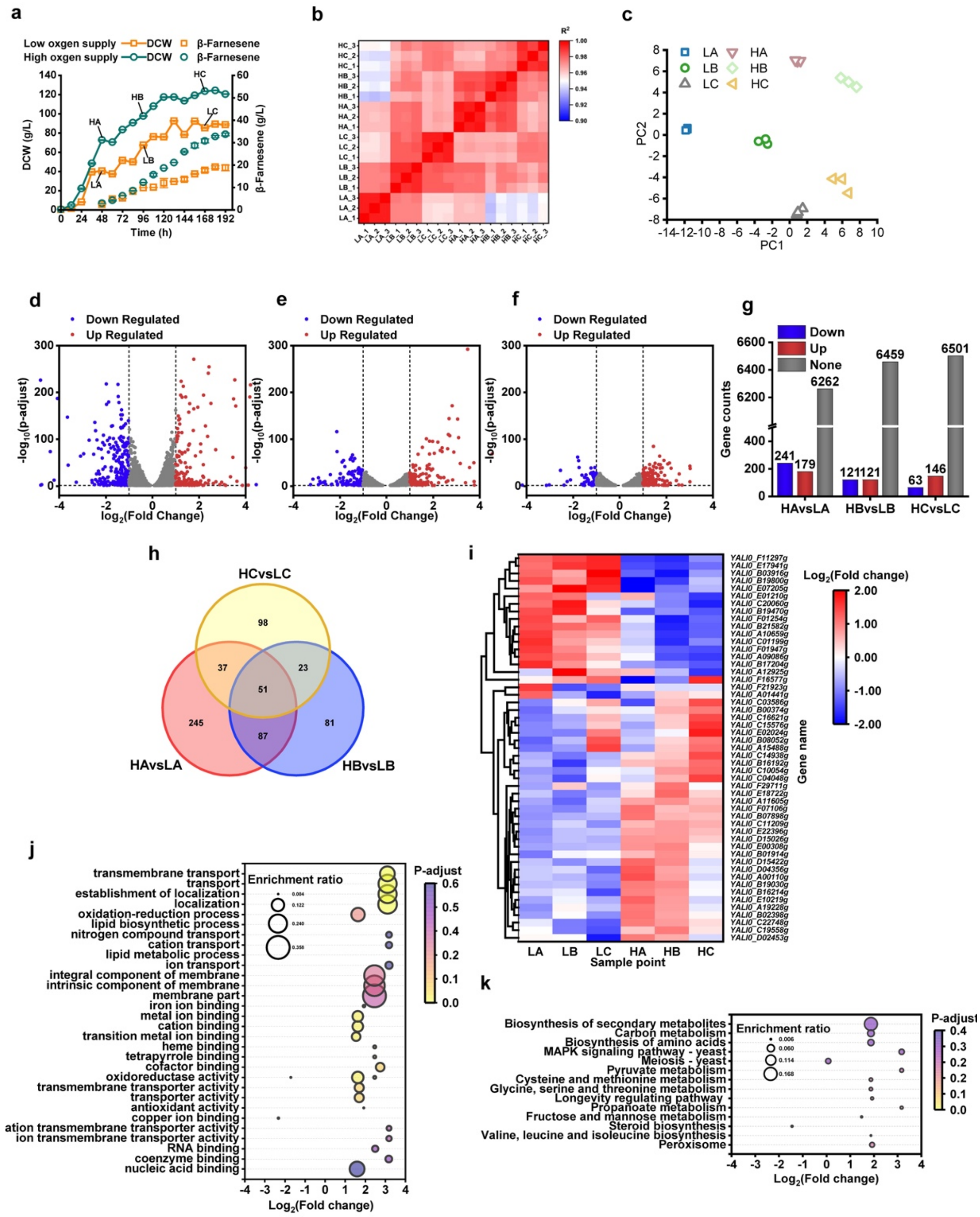
a
b
c
d
e
f
g
h
i
j
k
Low oxgen supply
High oxgen supply
DCW
β-Farnesene
Time (h)
Down Regulated
Up Regulated
log2(Fold Change)
HAvsLA
HBvsLB
HCvsLC
Gene counts
Sample point
Gene name
Log2(Fold change)
Enrichment ratio
P-adjust
PC1
PC2

Figure S6 Transcriptomic sequencing and analysis. a, Sampling point setting under different oxygen supply conditions, LA and HA represent low oxygen supply and high oxygen supply, respectfully. **b,** heat map of correlation between different samples. **c,** principal component analysis map. **d-f,** differential volcano map (from left to right represents sampling point A, B, C). **g,** Numbers of differential genes in different expression modes. **h,** differential expression venn map (51 genes differentially expressed throughout the whole cycle). **i,** cluster analysis heat map. **j-k,** Enrichment analysis of differential gene functions and metabolic pathways (**j**) GO database enrichment (**k**) enrichment of KEGG database. For **a,** the presented data reflects the mean ± standard deviation (n = 3).

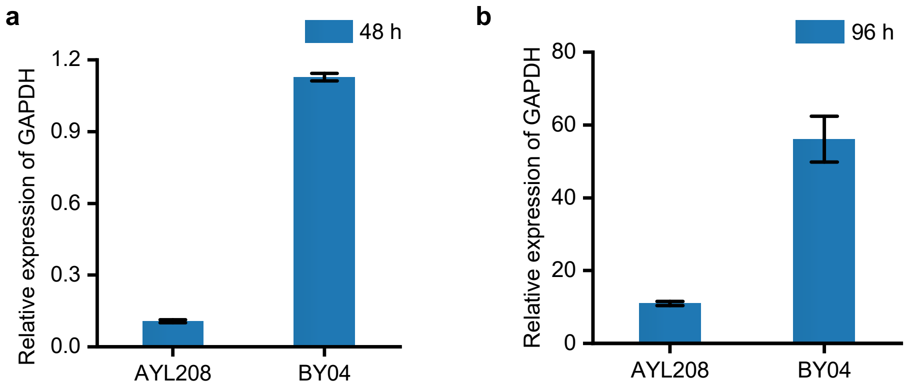

Figure S7 The expression level of *CHA1* relative to the reference gene *GAPDH*. a, expression level measured at 48 h. **b,** expression level measured at 96 h. The presented data reflects the mean ± standard deviation (n = 3)

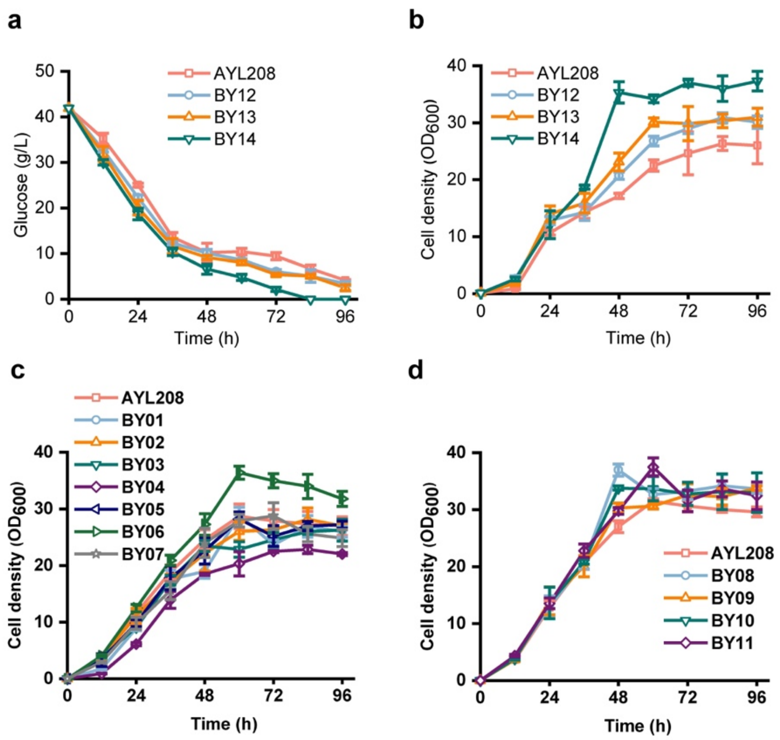

Figure S8 Fermentation performance in engineered strains. a-b, glucose consumption and cell density of strain AYL208 and BY12-14. **c-d,** cell density of strain AYL208 and BY01-BY11. The presented data reflects the mean ± standard deviation (n = 3)

Figure S9 The electron transport in the respiratory chain and the conversion of NADH to ATP, as well as their high demand during β-farnesene synthesis.

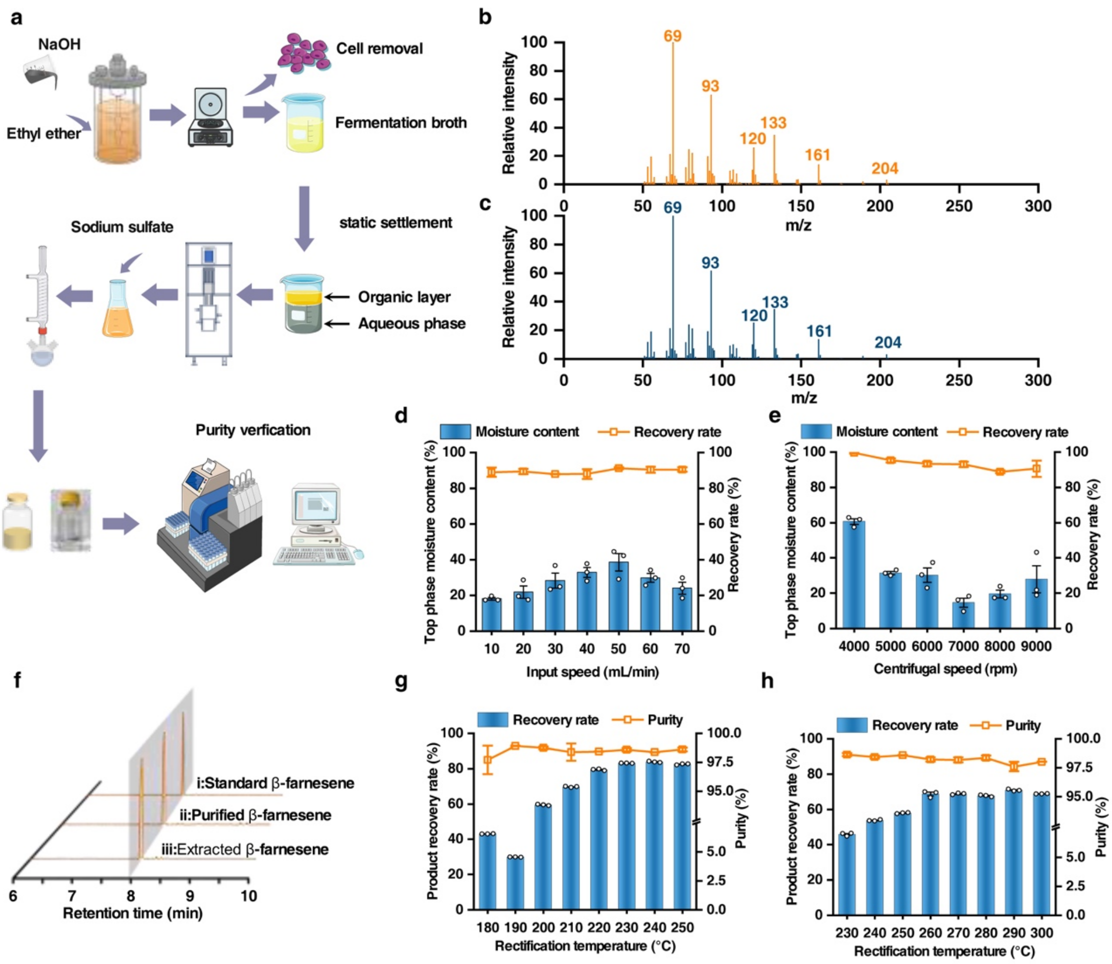

Figure S10 Isolation and purification of β-farnesene from fermentation broth. a, Outline of steps for the preparation and purification of β-farnesene. **b-c**, The mass spectrum profiles of purified sample (**b**) and the standard (**c**). **d-e,** Effect of different feed rates (**d**) and centrifuge speeds (**e**) on the moisture content in the top phase and organic phase recovery rate. **f,** The HPLC profiles of standard, purified and extracted samples. **g-h,** Effect of different rectification temperatures based on 4 mbar (**g**) and 14 mbar (**h**) on product recovery rate and purity.

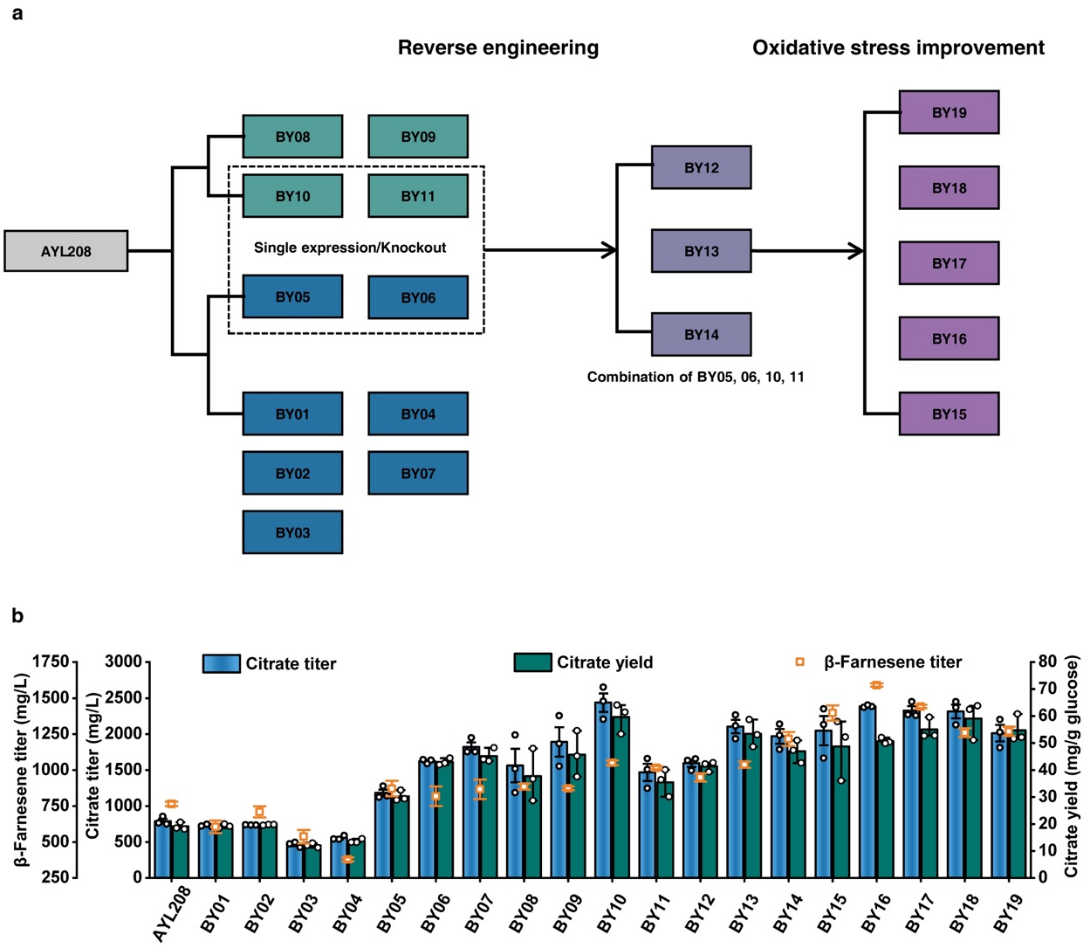

Figure S11 Strain construction and performance in shake flask fermentation. a, Flowchart of reconstructed strains with reverse engineering and oxidative stress improvement strategies. **b,** Citate titer, yield and β-farnesene titer from host strain AYL208 to BY19.

Table S1 Strains used in this study

Strains	**Genotype**	**Reference**
AYL208	PO1f, MVA pathway genes, ::*aaBFS*, ::*spHMGR*, intF4::P_{TEFin}-*mcMAE*-T_{xpr2}-P_{TEFin}-*mcMAE*-T_{xpr2}, intB3::P_{TEFin}-*mmACL*-T_{xpr2}-P_{TEFin}-*ylAMPD*-T_{xpr2}-P_{TEFin}-*ylYHM2*-T_{xpr2}, intA2::P_{TEFin}-anPK-T_{xpr2}-P_{TEFin}-bsuPTA-T_{xpr2}, Δ*ylPFK1*::3HA, pMO-P_{TEFin}-anPK-T_{xpr2}-P_{TEFin}-bsuPTA-$T_{xpr2,}$	[6]
BY01	AYL208, intD1::P_{TEFin}-*PUT4*-T_{lip2}	This work
BY02	AYL208, intD1::P_{TEFin}-*AMT3*-T_{lip2}	This work
BY03	AYL208, intD1::P_{TEFin}-*GAP2*-T_{lip2}	This work
BY04	AYL208, intD1::P_{TEFin}-*CHA1*-T_{lip2}	This work
BY05	AYL208, intD1::P_{TEFin}-*GRE2* -T_{lip2}	This work
BY06	AYL208, intD1::P_{TEFin}-*SOD2*-T_{lip2}	This work
BY07	AYL208, intD1::P_{TEFin}-*SOU1* -T_{lip2}	This work
BY08	AYL208, *GAP1*::3HA	This work
BY09	AYL208, *JEN1*::3HA	This work
BY10	AYL208, *ERG2*::3HA	This work
BY11	AYL208, *ALP1*::3HA	This work
BY12	AYL208, intD1::P_{TEFin}- *GRE2*-T_{xpr2}-P_{EXP}-*SOD2*-T_{lip2}	This work
BY13	AYL208, *ALP1*, *ERG2*::3HA	This work
BY14	AYL208, intD1::P_{TEFin}- *GRE2*-T_{xpr2}-P_{EXP}-*SOD2*-T_{lip2}, *ALP1*,	This work

	ERG2::3HA	
BY15	BY14, intF2::P_{TEFin}-*Vhb*-T_{lip2}	This work
BY16	BY14, intF2::P_{TEFin}-*YHB1*-T_{lip2}	This work
BY17	BY14, intF2::P_{TEFin}-*AHB1*-T_{lip2}	This work
BY18	BY14, intF2::P_{TEFin}-*Hbb-b2*-T_{lip2}	This work
BY19	BY14, intF2::P_{TEFin}-*HBZ*-T_{lip2}	This work

Table S2 Design parameters of agitators

Items	Impeller type	Leaf	angle of inclination	Blade width/length (mm)	Blade thickness (mm)	Insert stirring disc width (mm)	stirring disc diameter (mm)	diameter of axle (mm)
AS-4	Agitator (with straight blades)	4	0	14	1	6	40	8
AI-6	Agitator (with inclined blades)	6	45	14	1	6	40	8
AI-8	Agitator (with inclined blades)	8	45	14	1	6	40	8
AC-6	Agitator (with cambered blades)	6	(paraboloid: $y=\pm\frac{\sqrt{15x}}{2}$)	14	1	6	40	8

Table S3 The parameters of grids in the model

Impeller type	cells	faces	nodes
Agitator (with 4 straight blades)	1250002	2545311	231274
Agitator (with 6 inclined blades)	1484863	3023063	274436
Agitator (with 8 inclined blades)	2043019	4157529	376691
Agitator (with 6 cambered blades)	1278847	2603137	1278847

Table S4 Primers used in RT-qPCR

Primer	Sequences
GAPDH-F	GTCAACCTCGACGCCTACAA
GAPDH-R	ACCAGTGGAAGAGGGGATGA
CHA1-F	CCCCATCCCTAAAACCACCC
CHA1-R	GTTGTGTTTGTGTCGGTGGG

Table S5 Codon optimized genes in *Y.lipolytica* used in this study

Genes	Sequences
Vhb	ATGCTTGACCAGCAGACCATCAACATCATCAAGGCCACCGTGCCCG TGCTTAAAGAACATGGCGTGACCATTACCACCACCTTCTACAAGAA CCTGTTCGCCAAGCACCCTGAAGTGCGACCCCTGTTCGATATGGGC CGACAGGAGTCTCTGGAGCAGCCTAAAGCTCTGGCCATGACTGTTC TTGCTGCCGCCCAAAACATTGAAAACCTGCCCGCTATTCTGCCTGCC GTGAAGAAGATTGCCGTGAAGCACTGTCAAGCTGGAGTGGCTGCTG CTCACTACCCTATCGTGGGACAGGAACTGCTGGGAGCTATCAAGGA GGTGCTGGGAGATGCTGCCACCGATGACATTCTTGACGCCTGGGGA AAAGCCTATGGAGTGATCGCCGACGTGTTCATTCAGGTGGAGGCCG ATCTGTATGCTCAGGCCGTGGAGTAA
YHB1	ATGCTGGCTGAGAAGACCCGATCTATCATCAAGGCCACCGTGCCTG TGCTTGAACAACAAGGCACCGTGATTACCCGAACCTTCTACAAGAA CATGCTGACCGAGCACACCGAGCTGCTGAACATCTTCAACCGAACC AACCAGAAGGTGGGCGCTCAGCCTAATGCTCTGGCCACTACTGTTC TGGCTGCCGCTAAAAACATCGACGACCTGTCTGTGCTGATGGACCA CGTGAAGCAGATCGGCCACAAGCATCGAGCCCTGCAGATTAAGCCC GAGCACTACCCTATTGTGGGCGAGTACCTGCTGAAGGCCATCAAAG AGGTGCTGGGCGATGCTGCTACTCCCGAAATTATCAACGCCTGGGG CGAAGCTTACCAAGCCATCGCCGACATCTTCATCACCGTGGAGAAG AAGATGTACGAGGAGGCTCTGTGGCCTGGATGGAAGCCTTTTGACA

	TCACCGCCAAGGAGTACGTGGCCTCTGACATCGTGGAGTTCACCGT GAAGCCCAAGTTCGGCTCTGGAATCGAGCTGGAGTCTCTGCCTATT ACCCCCGGACAATACATCACCGTGAACACCCACCCTATCCGACAGG AGAACCAGTATGACGCCCTGCGACACTACTCTCTGTGCTCTGCCTCT ACCAAGAACGGACTGCGATTCGCCGTGAAAATGGAAGCCGCCCGA GAGAATTTTCCTGCCGGCCTGGTGTCTGAATACCTGCACAAGGATG CCAAAGTGGGCGACGAGATCAAACTGTCTGCTCCCGCTGGAGACTT TGCCATCAACAAGGAGCTGATCCACCAGAACGAAGTGCCTCTGGTG CTGCTGTCTTCTGGCGTGGGAGTGACTCCTCTGCTGGCTATGCTTGA GGAGCAGGTGAAGTGCAATCCCAACCGACCCATCTACTGGATCCAG TCTTCTTACGACGAGAAGACCCAGGCCTTCAAGAAGCACGTGGACG AGCTGCTTGCTGAGTGTGCCAATGTGGACAAGATCATCGTGCACAC CGACACTGAGCCTCTGATCAACGCCGCTTTCCTGAAGGAGAAGTCT CCTGCCCACGCCGATGTGTACACCTGTGGATCTCTGGCCTTCATGCA GGCTATGATCGGCCACCTGAAGGAGCTTGAACACCGAGATGACATG ATCCACTACGAACCCTTCGGCCCCAAGATGTCTACCGTGCAGGTGT AA
AHB1	ATGGAGTCTGAGGGCAAGATCGTGTTCACCGAGGAGCAAGAAGCC CTGGTGGTGAAGTCTTGGTCTGTGATGAAGAAGAACTCTGCCGAGC TGGGCCTGAAGCTGTTCATCAAGATCTTCGAGATCGCCCCCACCAC CAAGAAGATGTTCTCTTTCCTGCGAGACTCTCCTATCCCCGCTGAGC AAAACCCCAAACTGAAGCCCCACGCCATGTCTGTGTTCGTGATGTG

	CTGCGAGTCTGCCGTGCAACTTCGAAAGACCGGCAAAGTGACCGTG AGAGAGACTACCCTGAAAAGACTGGGCGCCTCTCACTCTAAATACG GCGTGGTGGACGAACATTTCGAGGTGGCTAAGTACGCCCTGCTGGA GACTATTAAGGAGGCCGTGCCCGAAATGTGGTCCCCCGAGATGAAA GTGGCTTGGGGCCAGGCCTATGATCATCTGGTGGCCGCTATTAAGG CCGAGATGAACCTGTCTAACTAA
Hbb-b2	ATGGTGCATCTTACCGACGCCGAGAAGTCTGCTGTGTCTTGCCTGTG GGCTAAGGTGAATCCCGATGAGGTGGGCGGAGAAGCTCTTGGAAG ACTGCTGGTGGTGTACCCTTGGACCCAGCGATACTTCGACTCTTTCG GCGACCTGTCTTCTGCCTCTGCCATCATGGGAAACCCCAAGGTTAA GGCCCACGGCAAGAAAGTGATCACCGCCTTCAACGAGGGCCTGAA GAACCTGGACAACCTGAAGGGCACCTTCGCCTCTCTGTCTGAGCTG CACTGTGACAAGCTTCATGTGGACCCCGAGAACTTTAGACTGCTGG GCAACGCTATCGTTATCGTGCTGGGCCATCATCTGGGCAAAGACTT CACCCCTGCCGCTCAAGCTGCTTTCCAGAAGGTGGTGGCTGGAGTG GCTACTGCTCTGGCCCATAAGTACCACTAA
HBZ	ATGTCTCTGACCAAGACCTAAGGCACCATCATCGTGTCTATGTGGG CCAAGATCTCTACCCAGGCCGATACCATTGGCACCGAGACTCTGGA GCGACTGTTCCTTTCTCACCCCCAGACCAAGACTTACTTCCCCCACT TCGATCTGCATCCTGGCTCTGCTCAACTTAGAGCCCATGGCTCTAAG GTGGTGGCTGCTGTTGGAGATGCCGTGAAGTCTATCGACGATATCG GCGGCGCCCTGTCTAAACTGTCTGAGCTGCACGCCTACATCCTGAG

	AGTGGACCCCGTGAACTTCAAGCTGCTGTCTCACTGTCTGCTGGTG ACTCTGGCTGCCAGATTCCCTGCTGACTTCACCGCTGAGGCTCATGC TGCTTGGGCCAAGTTTCTGTCTGTGGTGTCTTCTGTGCTGACCGAGA AGTACCGATAA

Table S6 Differentially expressed genes during the fermentation

Gene name	Gene length	Biofunction
YALI0A00110p	2619	Oligopeptide transporter
YALI0A01441p	1065	Epoxide hydrolase
YALI0A09086p	447	Regulates cell cycle initiation
YALI0A10659p	909	ATP carrier protein
YALI0A11605p	1605	MFS transporter
YALI0A12925p	1137	/(Undefined)
YALI0A15488p	1581	Cytochrome P450
YALI0A19228p	1368	Ammonium transporter
YALI0B00374p	1170	Acid protease
YALI0B01914p	1755	Transporter
YALI0B02398p	2415	Oligopeptide transporter
YALI0B03916p	564	Peptide methionine sulfoxide reductase
YALI0B07898p	2847	Oligopeptide transporter
YALI0B08052p	1041	oxidoreductase
YALI0B16192p	837	NADP-dependent mannitol dehydrogenase
YALI0B16214p	1095	L-serine dehydratase/L-threonine deaminase
YALI0B17204p	657	sterol isomerase
YALI0B19030p	927	/(Undefined)
YALI0B19470p	1590	Carboxylic acid transporter protein
YALI0B19800p	1809	amino-acid permease

YALI0B21582p	858	zinc finger domain transcription factor
YALI0C01199p	1071	/(Undefined)
YALI0C03586p	2112	/(Undefined)
YALI0C04048p	1293	/(Undefined)
YALI0C10054p	1566	Cytochrome P450
YALI0C11209p	342	/(Undefined)
YALI0C14938p	1344	Acid protease
YALI0C15576p	696	/(Undefined)
YALI0C16621p	621	Superoxide dismutase
YALI0C19558p	606	/(Undefined)
YALI0C20060p	159	Metallothionein-2
YALI0C22748p	1188	Lovastatin esterase
YALI0D02453p	360	Ethanolamine utilization protein
YALI0D04356p	1245	/(Undefined)
YALI0D15026p	1824	Major Facilitator Superfamily
YALI0D15422p	1623	Proline-specific permease
YALI0E00308p	1773	Lysine histidine transporter
YALI0E01210p	1038	/(Undefined)
YALI0E02024p	3375	/(Undefined)
YALI0E07205p	1602	GABA-specific permease
YALI0E10219p	1782	amino-acid permease
YALI0E17941p	873	Lytic transglycolase

YALI0E18722p	1899	/(Undefined)
YALI0E22396p	564	/(Undefined)
YALI0F01254p	1671	amino-acid permease
YALI0F01947p	1350	β-glucosidase btgE
YALI0F07106p	1737	Lysine histidine transporter
YALI0F11297p	930	Methylsterol monooxygenase
YALI0F16577p	906	Phosphatidylinositol transfer protein SFH5
YALI0F21923p	645	/(Undefined)
YALI0F29711p	1743	Protein HOL1

Table S7 Differentially expressed genes used in strain modification

Model	Strain	Symbol name	Protein names	Function
UP	BY01	*PUT4*	*YALI0D15422p*	Proline and gamma-aminobutyrate permease
	BY02	*AMT3*	*YALI0A19228p*	Ammonium transporter
	BY03	*GAP2*	*YALI0E10219p*	General amino acid permease
	BY04	*CHA1*	*YALI0B16214p*	L-serine/L-threonine deaminase
	BY05	*SOU1*	*YALI0B16192p*	Sorbitol utilization protein
	BY06	*SOD2*	*YALI0C16621p*	Superoxide dismutase (Mn)
	BY07	*GRE2*	*YALI0B08052p*	NADPH-dependent methylglyoxal reductase
Down	BY08	*GAP1*	*YALI0B19800p*	General amino acid permease
	BY09	*JEN1*	*YALI0B19470p*	Carboxylic acid transporter protein singleton
	BY10	*ERG2*	*YALI0B17204p*	C-8 sterol isomerase singleton
	BY11	*ALP1*	*YALI0F01254p*	High-affinity permease for basic amino acids

Table S8 Stoichiometric equation for actual production of engineered strains

Strain	Equation
AYL208	22.76 $C_6H_{12}O_6$+ 101.89 O_2→ $C_{15}H_{24}$+ 36.76 $CH_{1.6}O_{0.54}N_{0.14}$ + 119.12 CO_2+107.17 H_2O
BY16	15.44 $C_6H_{12}O_6$+ 67.22 O_2→ $C_{15}H_{24}$+ 17.325 $CH_{1.6}O_{0.54}N_{0.14}$ + 65.91 CO_2+ 65.45 H_2O

Supplemental Reference

1 U. von Stockar, J.-S. Liu, Biochim. Biophys. *Acta, Bioenerg.*,1999,**1412**,191-211.

2 J. Xu, N. Liu, K. Qiao, S. Vogg, G. Stephanopoulos, *Proc. Natl. Acad. Sci.*, 2017, **114**, E5308–E5316.

3 C. Verduyn, *Antonie van Leeuwenhoek*, 1991, **60**, 325-253.

4 H. M. van Rossum, B. U. Kozak, J. T. Pronk, A. J. A. van Maris, *Metab. Eng.*, 2016, **36**, 99–115.

5 A. L. Meadows, K. M. Hawkins, Y. Tsegaye, E. Antipov, Y. Kim, L. Raetz, R. H. Dahl, A. Tai, T. Mahatdejkul-Meadows, L. Xu, L. Zhao, M. S. Dasika, A. Murarka, J. Lenihan, D. Eng, J. S. Leng, C.-L. Liu, J. W. Wenger, H. Jiang, L. Chao, P. Westfall, J. Lai, S. Ganesan, P. Jackson, R. Mans, D. Platt, C. D. Reeves, P. R. Saija, G. Wichmann, V. F. Holmes, K. Benjamin, P. W. Hill, T. S. Gardner, A. E. Tsong, *Nature*, 2016, **537**, 694–697.

6 H. Bi, C. Xu, Y. Bao, C. Zhang, K. Wang, Y. Zhang, M. Wang, B. Chen, Y. Fang, T. Tan, *Bioresour. Technol*., 2023, **382**, 129171.